Methotrexate Pharmacokinetics

K. B. BISCHOFF*‡, R. L. DEDRICK*, D. S. ZAHARKO†, and J. A. LONGSTRETH*

Abstract □ A pharmacokinetic model is presented to predict the detailed distribution and excretion of methotrexate in several mammalian species over a wide range of doses. Anatomical compartments include liver, kidneys, gastrointestinal tract, muscle, and plasma; multicompartment representations simulate biliary excretion and movement of drug through the gastrointestinal tract with partial reabsorption. Tissue-to-plasma distribution coefficients include linear and strong saturable (presumed dihydrofolate reductase) effects. Required parameters are measured directly or estimated on the basis of physiological principles for mice, rats, dogs, and man.

Keyphrases □ Methotrexate pharmacokinetics—model, mammals □ Tissue/plasma distribution coefficients—methotrexate, mammals □ Pharmacokinetic parameters—methotrexate absorption, distribution, excretion □ Dihydrofolate reductase binding—methotrexate □ Model, methotrexate distribution, mammals—one, two compartments

A previous paper (1) described a preliminary mathematical model for methotrexate pharmacokinetics in mice. Since it was based on only one dose level, many of its conclusions were, necessarily, tentative. This paper describes much more extensive work at a variety of dose levels with several species, including man. The same general rationale proposed in previous studies (1–3) is utilized, namely, basing the model, as much as possible, on established, independently verifiable, physiological concepts. It is important to emphasize this approach since, in this fashion, one can obtain pharmacokinetic models that provide generally applicable *a priori* predictions of drug distribution behavior. Specific details will be given with the model description.

Cancer chemotherapeutic agents are usually screened for activity against a limited number of tumor systems in the mouse and rat. If their activity is sufficient to warrant further investigation, they are tested for toxicity in a variety of animal species. Detailed information is developed on quantitative and qualitative toxicology as well as the pharmacologic distribution and metabolic fate. The most promising drugs are then evaluated clinically in man.

The fundamental issues of drug toxicity include both the physical aspects of drug distribution within the body and drug effect at particular sites of action. Experience to date indicates that the dynamics of drug distribution in the body can often be *predicted* on the basis of fundamental information on physicochemical properties, transport, metabolism, and various excretory mechanisms. The method is analogous to that used for "scale-up" for a chemical plant where rational design can be based on laboratory data applied according to reasonably well-established techniques. Application of this concept to pharmacokinetic modeling should permit the quantitation of interspecies differences with respect to drug distribution and prediction of drug concentration at specific sites as functions of dose schedule and route of administration. Reliable prediction can enable more effective drug screening and enhance the ability of the clinician to devise optimum therapeutic regimens. The latter is of particular concern for antineoplastic drugs for which therapeutic effect and toxicity must be balanced carefully.

BASIS AND DEVELOPMENT OF MODEL

The model employs the lumped compartmental approach with the restriction that the volumes, flows, and other properties be physiologically meaningful and usually independently measured. The concept of flow-limited conditions is used for all body regions. If quantitative membrane permeabilities were more readily available, other cases could be considered, but this does not seem feasible at present.

Many of the broad features described earlier (1) are valid following intravenous injection of methotrexate: (*a*) a very rapid drop in plasma concentration and an increase in gut-lumen concentration, suggesting the importance of tissue uptake and biliary secretion; (*b*) a peak gut-lumen/plasma concentration ratio of about 100; and (*c*) linear binding of methotrexate by tissues at plasma concentrations above 0.1 mcg./ml. At low concentration levels, the binding became nonlinear (4), presumably because of the strong binding to dihydrofolate reductase.

The basic model, incorporating the important enterohepatic circulation, is shown in Fig. 1. The various symbols are defined in the

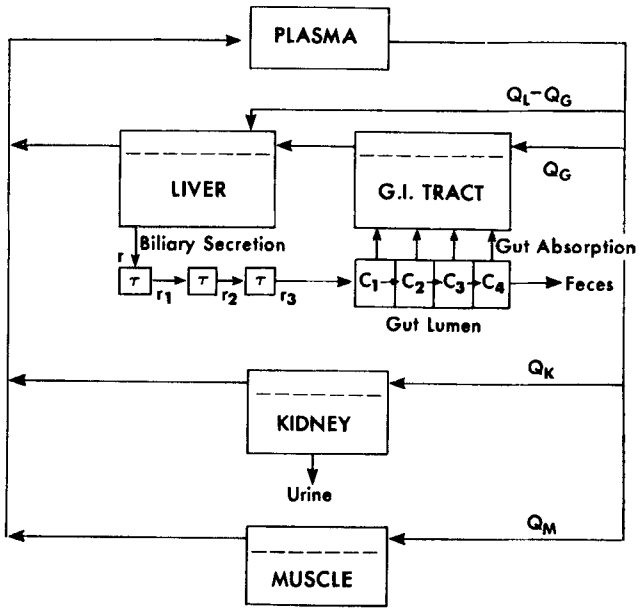

Figure 1—*Body compartments important in methotrexate distribution.*

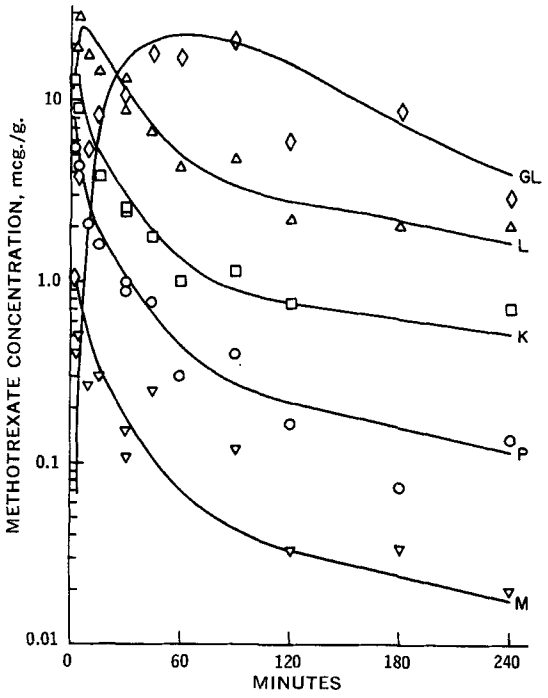

Figure 2—*Model prediction* versus *experimental results, mice, 3 mg./kg. i.v. Solid lines are model predictions; symbols are experimental data. Key:* GL(◇), *small intestine;* L(△), *liver;* K(□), *kidney;* P(○), *plasma; and* M(▽), *muscle.*

Nomenclature section. Two rather unique features need to be described in more detail—the "multicompartment" models used for the biliary secretion process and for the gut lumen. In the previous study (1), a mathematical time-delay or step function was used to simulate the bile formation and secretion time in the liver. In other words, a period of about 5 min. (in mice) was allowed before the drug in the bile was introduced into the gut lumen. This abrupt introduction caused this portion of the gut-lumen-predicted curve to overshoot the actual data, and a smoother representation of the real "S-shaped" bile concentration efflux curve was desired. A finite series of discrete compartments is able to do this, as is commonly done in chemical engineering for similar situations (5). A more extensive description and test of this scheme to represent bile function are given elsewhere (6), and it was found materially to improve the present model predictions.

The transit of drug down the gut is handled similarly, except that provision for transport through the intestinal wall is made. This concept, rather than a single compartment with time delay, is used again to provide a smooth response. Also, rather than a well-mixed uniform region, the tubular nature of the gut lumen must be accounted for to simulate the proper concentration appearing in the feces. This is done by having the feces "exit" from the last gut-lumen region. The rigorous details of properly accounting for binding, *etc.*, were given previously (1). The complete set of mass balance equations for the various anatomical body regions can be written as follows.

Plasma:

$$V_P \frac{dC_P}{dt} = Mg(t) + Q_L \frac{C_L}{R_L} + Q_K \frac{C_K}{R_K} + Q_M \frac{C_M}{R_M} - (Q_L + Q_K + Q_M)C_P \quad \text{(Eq. 1)}$$

Muscle:

$$V_M \frac{dC_M}{dt} = Q_M \left(C_P - \frac{C_M}{R_M}\right) \quad \text{(Eq. 2)}$$

Kidney:

$$V_K \frac{dC_K}{dt} = Q_K \left(C_P - \frac{C_K}{R_K}\right) - k_K \frac{C_K}{R_K} \quad \text{(Eq. 3)}$$

Liver:

$$V_L \frac{dC_L}{dt} = (Q_L - Q_G)\left(C_P - \frac{C_L}{R_L}\right) + Q_G \left(\frac{C_G}{R_G} - \frac{C_L}{R_L}\right) - r \quad \text{(Eq. 4)}$$

where:

$$r \equiv \frac{k_L(C_L/R_L)}{K_L + (C_L/R_L)} \quad \text{(Eq. 5)}$$

Equation 5 defines the secretion rate (mcg./min.) of methotrexate out of the liver cells into the bile ducts, and it allows for potential saturation effects (which were not observed at any dose levels studied).

$$\tau \frac{dr_1}{dt} = r - r_1 \quad \text{(Eq. 6}a\text{)}$$

$$\tau \frac{dr_2}{dt} = r_1 - r_2 \quad \text{(Eq. 6}b\text{)}$$

$$\tau \frac{dr_3}{dt} = r_2 - r_3 \quad \text{(Eq. 6}c\text{)}$$

Equations 6*a–c* are balanced directly on the secretion rate; the only model parameter involved is the holding time, τ. Three compartments are adequate to model separate experiments where the bile duct is cannulated and the bile concentration of methotrexate is directly measured.

Gut tissue:

$$V_G \frac{dC_G}{dt} = Q_G \left(C_P - \frac{C_G}{R_G}\right) + \sum_{i=1}^{4} \frac{1}{4} \left(\frac{k_G C_i}{K_G + C_i} + bC_i\right) \quad \text{(Eq. 7}$$

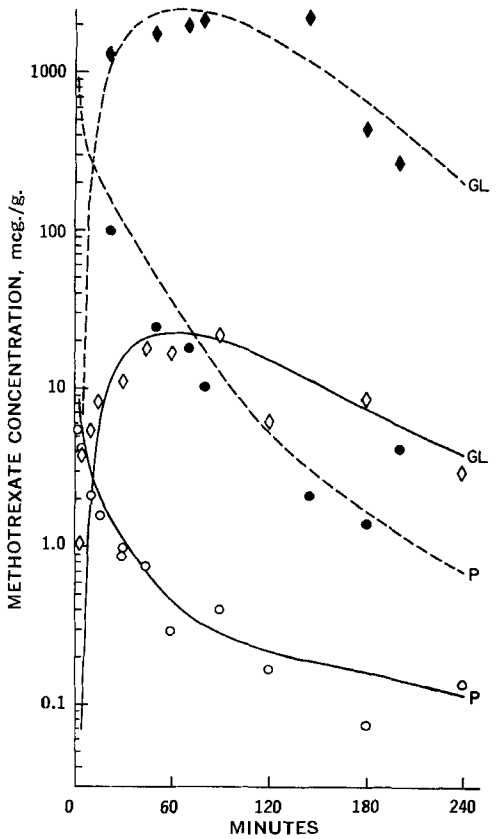

Figure 3—*Model prediction* versus *experimental results, mice. Empty symbols are 3 mg./kg.; solid symbols are 300 mg./kg. i.v. See Fig. 2 for symbol key.*

Table I—Model Parameters for Methotrexate in Several Species

Parameter	Mouse	Rat	5 kg., Dog/Monkey	17 kg., Dog	Man
Body weight, g.[a]	22	200	5000	17,000	70,000
Volume, ml.[b]					
V_P	1.0	9.0	220	650	3,000
V_M	10.0	100	2500	7,500	35,000
V_K	0.34	1.9	30	76	280
V_L	1.3	8.3	135	360	1,350
V_G[c]	1.5	11.0	230	640	2,100
V_{GL}[c]	1.5	11.0	230	640	2,100
Plasma flow rate, ml./min.[b]					
Q_M	0.5	3.0	50	140	420
Q_K	0.8	5.0	74	190	700
Q_L	1.1	6.5	92	220	800
Q_G	0.9	5.3	75	190	700
Tissue/plasma equilibrium distribution ratio for linear binding[d,e]					
R_M	0.15	0.15	(0.15)	(0.15)	(0.15)
R_K	3.0	3.0	(14)	14	(3.0)
R_L	10	3.0	(2.0)	2.0	(3.0)
R_G	1.0	(1.0)	(1.0)	(1.0)	(1.0)
Strong specific binding[e]					
a_M	0.0	0	(0)	(0)	(0)
a_K	0.3	0.3	(0.3)	(0.3)	(0.3)
a_L	0.3	0.5	(0.4)	(0.4)	(0.4)
a_G	0.1	(0.1)	(0.1)	(0.1)	(0.1)
Kidney clearance, ml./min.[d,e]					
k_K	0.2	1.1	(20)	56	190[f]
Bile secretion parameters[d,e]					
Clearance = k_L/K_L, ml./min.[g]	0.4	3.0	(2.0)	8	200[h]
τ, min.	2.0	2.0	(6)	8.0	(10)
Gut-lumen parameetrs[e]					
Transit time, min.	100	100[i]	(450)	(650)	(1,000)
Reciprocal = k_F, min.$^{-1}$	0.01	0.01	(0.0022)	(0.0015)	(0.001)
k_G, mcg./min.	0.20	(20)	(340)	(1,000)	(1,900)
K_G, mcg./ml.	6.0	(200)	(200)	(200)	(200)
b, ml./min.	0.001	—	—	—	—

[a] "Standard" values (average). [b] Based on physiological information; see *Appendix*. [c] Gut and gut-lumen volumes not independently measured, *i.e.*, gut-lumen "concentrations" are effective values. [d] Measured experimentally; see text. [e] Values in parentheses are estimates. [f] Liegler *et al.* (15). [g] Only the ratio k_L/K_L is needed, since no saturation was observed; so K_L is very large. [h] Conjectural value to create best fit to data. [i] Compare Sikov *et al.* (16).

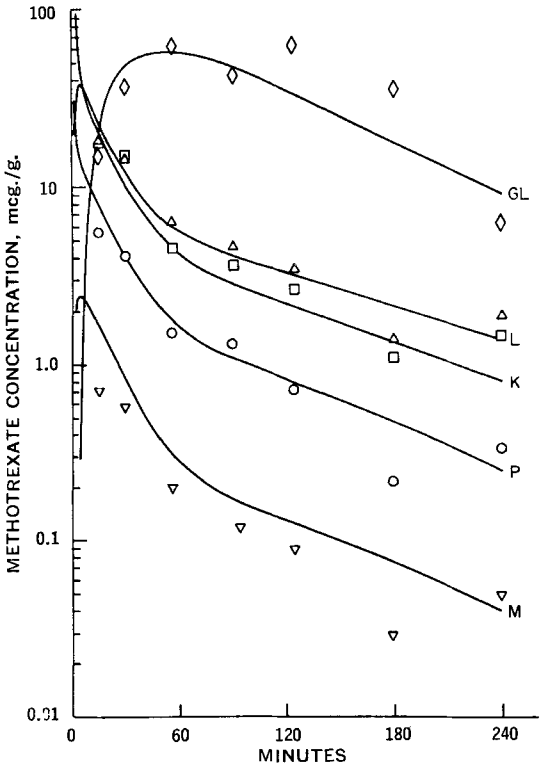

Figure 4—*Model prediction* versus *experimental results, rats, 6 mg./kg. i.p. See Fig. 2 for symbol key.*

Gut lumen:

$$\frac{dC_{GL}}{dt} = \frac{1}{4}\sum_{i=1}^{4}\frac{dC_i}{dt} \qquad \text{(Eq. 8}a\text{)}$$

$$\frac{V_{GL}}{4}\frac{dC_1}{dt} = r_3 - k_F V_{GL} C_1 - \frac{1}{4}\left(\frac{k_G C_1}{K_G + C_1} + bC_1\right) \qquad \text{(Eq. 8}b\text{)}$$

$$\frac{V_{GL}}{4}\frac{dC_i}{dt} = -k_F V_{GL}(C_{i-1} - C_i) - \frac{1}{4}\left(\frac{k_G C_i}{K_G + C_i} + bC_i\right) \quad (i = 2,3,4) \qquad \text{(Eq. 8}c\text{)}$$

In Eqs. 7 and 8, the last terms represent gut absorption from the lumen to the tissue (and blood flow), with the possibility of both saturable $[(k_G C_i/K_G + C_i)]$ and nonsaturable (bC_i) effects. Both effects may be important for folic acid (7, 8) and, therefore, may apply to methotrexate, since both substrates were reported to use the same transport system (9). The four regions are judged sufficient to model the gut-lumen response. The absorption characteristics are assumed the same for all segments because of a lack of more detailed information; other complications, such as location-dependent absorption, could be accounted for. Upon substitution of suitable numerical values for the various parameters, these equations can be solved by a computer.

PARAMETER VALUES

Many of the parameters for mice, as given earlier (1), are retained here, except for the case of the zero-order gut absorption. This was reasonable for the one dose of 3 mg./kg., but the simulation was inadequate for a wider range of dose levels. The justification for the assumption of zero-order absorption (1) was the apparent leveling of

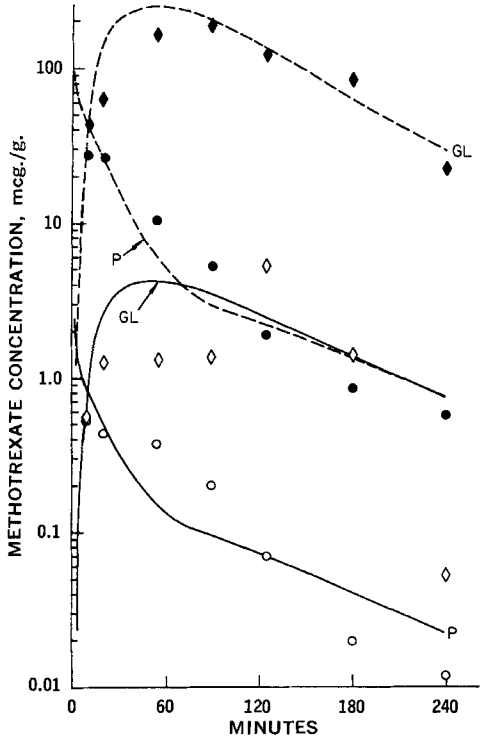

Figure 5—*Model prediction* versus *experimental results, rats. Empty symbols are 0.5 mg./kg.; solid symbols are 25 mg./kg. i.p. See Fig. 2 for symbol key.*

the plasma concentration after 2–3 hr. However, since it was found (10) that significant intestinal metabolism eventually occurs, the reliability of the measured radioactivity at these longer times is questionable. Strong binding to dihydrofolate reductase is also a complication. Thus, even though a definitive model for gut absorption is still not available, it is apparently not readily saturable. Therefore, the model accounts for both saturable and nonsaturable absorption in Eqs. 7 and 8.

The simple physiological parameters of organ volumes and flows for other animal species are detailed in the *Appendix*. Although the

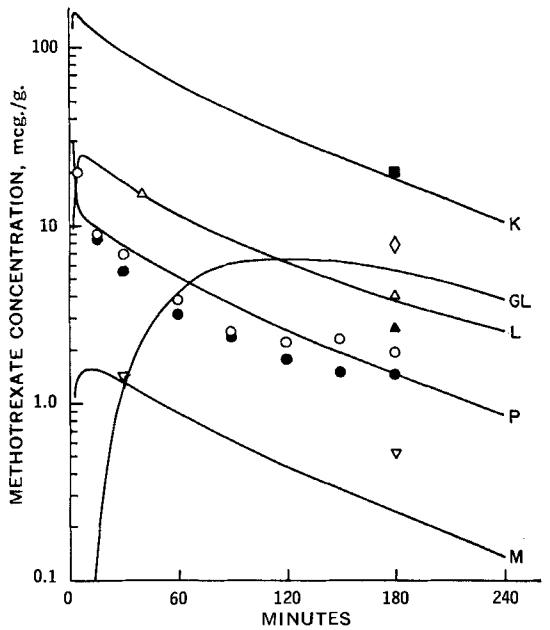

Figure 6—*Model prediction* versus *experimental results. Two experiments, dogs, 3 mg./kg. i.v., represented by empty and solid symbols. See Fig. 2 for symbol key.*

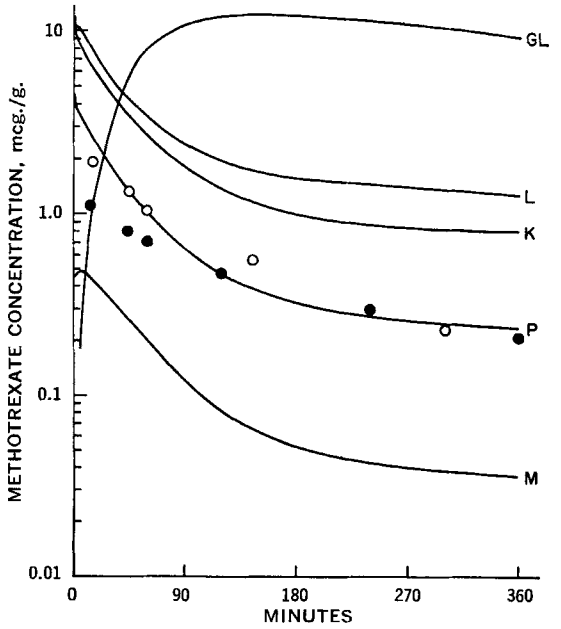

Figure 7—*Man, 1 mg./kg. i.v. Dark and clear symbols are results of two separate experiments. See Fig. 2 for symbol key (12).*

kidney clearance is close to inulin, it is specifically determined for methotrexate by comparing the time integral of the plasma concentration with cumulative urine formation after intraperitoneal or intravenous injections of the drug. The tissue/plasma equilibrium ratios are derived by some constant-infusion experiments and/or the portion of the intravenous pulse injection curve after the initial redistribution. For high concentrations, they are constants, indicating linear binding; for low concentrations, they are given by the sum of this linear nonspecific binding (RC_P) and strong binding (a), presumed to be associated with dihydrofolate reductase, according to:

$$C_{\text{tissue}} = RC_P + \frac{aC_P}{\epsilon + C_P} \qquad \text{(Eq. 9)}$$

The magnitude of ϵ may be estimated from the work of Werkheiser (11), who found that the dissociation constant of the enzyme–drug complex is less than 1.5×10^{-10} M for a noncompetitive inhibitor or

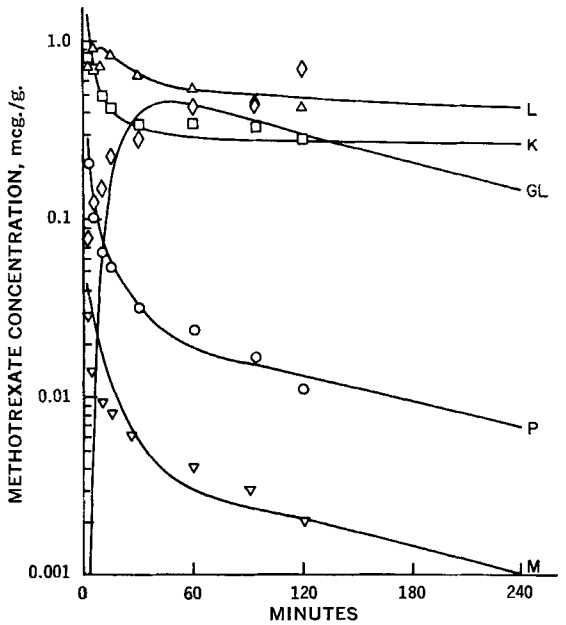

Figure 8—*Model prediction* versus *experimental results, mice, 0.12 mg./kg. See Fig. 2 for symbol key.*

less than 3×10^{-11} M for a competitive inhibitor. Thus, ϵ is of the order of 10^{-5} mcg./ml. or less. At the plasma concentrations studied, therefore, the binding to dihydrofolate reductase may be considered stoichiometric.

For high values of C_P, the second term in Eq. 9 is much smaller than the first, since a is much less than RC_P and ϵ is very much less than C_P. Thus, RC_P dominates, and the binding may be considered linear. For small values of C_P, however, the second term in Eq. 9 becomes important.

The bile clearance is determined by separate experiments, except where indicated, and the complete set of parameter values used in the simulations to be described is given in Table I.

SIMULATIONS AND COMPARISONS WITH DATA

The model parameters in Table I are used in Eqs. 1–9 for simulations of various dose levels and animal species. The values presented in Table I were used for *all* dose levels so that the model would achieve real physiological meaning.

Figure 2 compares the model results in several body regions with experimental data for 3 mg./kg. in the mouse. The results are in good agreement, similar to those reported earlier (1) for the preliminary model, except for a better gut-lumen simulation; also, the curves do not level out. Figure 3 gives the results for two high doses, 3.0 and 300 mg./kg. Other tissues are not presented in order to simplify the figure; however, they were also predictable and followed the same time course as plasma (Fig. 2).

The same types of results are given for rats in Figs. 4 and 5, showing fair agreement. Although the trend of the gut-lumen concentration is predictable, there is more variability in the data obtained at the low dose. Figure 6 illustrates the comparisons for a small amount of dog data, and the results are reasonably good. Finally, Fig. 7 compares the plasma results for man with model predictions and also gives predicted values for the other body regions. The prediction of 57% of the total dose in the urine at 4 hr. may be compared with the observed value range of 38–75% observed by Henderson *et al.* (12) at the same dose level; corresponding values for 24 hr. are: predicted, 87%; and observed, 75–88%. Based on these illustrations, the model does a reasonable job of predicting the methotrexate distribution for all the species at the fairly high dose levels ($\geq$1 mg./kg.). More extensive specific clinical experiments would be useful for more confidence in the parameter values for man.

The case of very low doses is of interest here because it illustrates the effect of the nonlinear strong binding in Eq. 9. The kinetics of distribution in various body tissues are also of practical importance to dermatologists, since such low doses are used to treat psoriasis (13). Figure 8 shows the predicted and measured tissue concentrations following an intravenous dose of 0.12 mg./kg. in the mouse. Comparison with Fig. 2 (3 mg./kg.) shows clearly the effect of the strong binding in the liver and kidney at the low dose. The plasma concentration falls rapidly in very short times, while a large fraction of the dose is bound to these tissues. As the plasma concentration continues falling, the concentrations in the liver and kidney remain high. As suggested by Werkheiser (11), other dihydrofolate reductase-containing tissues no doubt behave in a similar manner. There is evidence that dihydrofolate reductase inhibitors exhibit strong saturable binding in human liver, kidney, and small intestine which persists for days but which can be dissociated by a high dose of nonlabeled drug (14).

CONCLUSIONS

A mathematical model is presented which predicts detailed distribution of methotrexate in the tissues of several mammalian species. It is based on anatomical compartments and intercompartment flow transport. Tissue-to-plasma distribution coefficients include provision for strong binding to dihydrofolate reductase. The drug is cleared from the plasma by the kidney and excreted in the bile, with subsequent partial intestinal reabsorption. At present, the greatest uncertainty is in the exact kinetics to describe intestinal absorption in the intact animal. The model contains multicompartment descriptions of the biliary system and the intestine based on physiologic principles. Phenomena, such as local differences in intestinal absorption, could be incorporated if sufficient data were available.

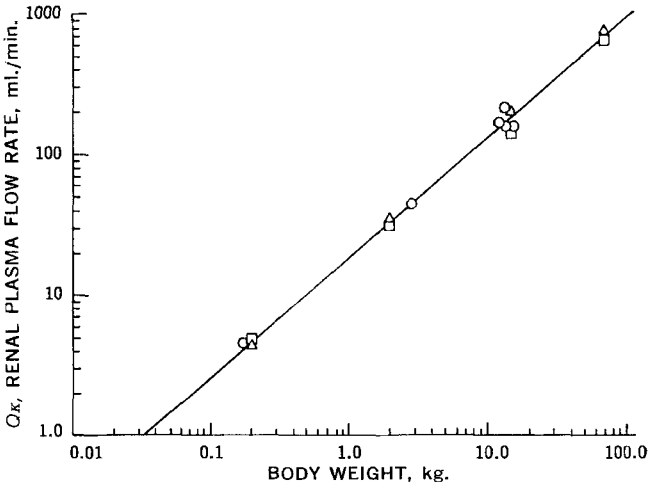

Figure A1—*Renal plasma flow rate. Data sources:* ○, Reference 20, *p. 127; and* △, □, Reference 21, *p. 1483.*

The same model is used for the mouse, rat, dog, and human, with specific parameters chosen for the species to be simulated. The model predicts tissue concentrations in the subhuman species and also predicts observed plasma concentrations and urinary and fecal excretion in man.

NOMENCLATURE

a	= strong specific binding, mcg./g.
b	= rate constant for nonsaturable gut absorption, ml./min.
C	= drug concentration, mcg./g. or mcg./ml.
$g(t)$	= injection function, min.$^{-1}$
k_F	= reciprocal of nominal transit time in small intestine, min.$^{-1}$
k_G	= saturable rate of intestinal absorption, mcg./min.
k_K	= clearance by kidney, ml./min.
k_L	= saturable rate of drug transport into bile, mcg./min., Eq. 5
K	= constant of Michaelis form for intestinal absorption or bile formation, mcg./ml.
M	= amount of drug, mcg.
Q	= plasma flow rate, ml./min.
r	= drug-transport rate in bile, mcg./min.
R	= tissue-to-plasma equilibrium distribution ratio for linear binding, dimensionless
R'	= variable tissue-to-plasma equilibrium distribution ratio including effect of strong specific binding
t	= time, min.
V	= volume of compartment, ml.
W	= body weight, kg.
ϵ	= dissociation constant of enzyme–inhibitor complex, mcg./ml., Eq. 9
τ	= nominal residence time in bile subcompartment, min.

Subscripts

G	= gastrointestinal tract
GL	= gut lumen
K	= kidney
L	= liver
M	= muscle
P	= plasma
tissue	= G, K, L, or M
1, 2, . . .	= bile or gut-lumen subcompartments

APPENDIX

This section briefly summarizes the literature data used for the physiological values of organ volumes and flows.

The volumes are essentially taken from the correlations of Adolph (17) and spot-checked with some of the authors' own organ weight data and that of Mapleson (18) and Crile and Quiring (19). Adolph (17) gives $(V_{Bl})_{Adolph} = 0.055\ (1000W)^{0.99}$, where the volume is in milliliters (grams for density of 1.0 g./ml.) and the body weight, W, is in kilograms. For a standard man of 70 kg., $(V_{Bl})_{Adolph} = 3500$.

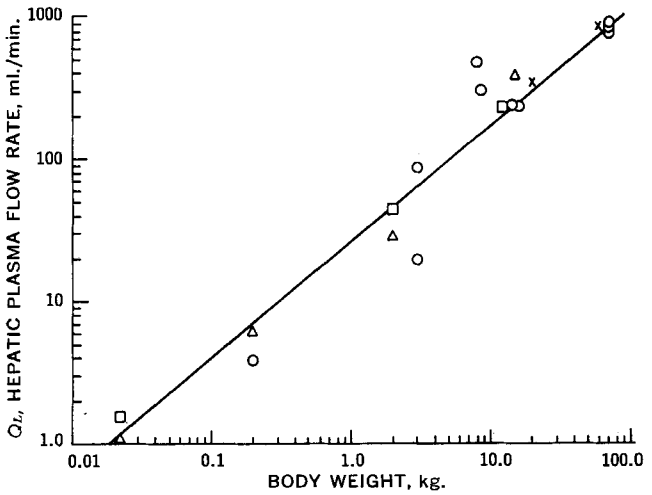

Figure A2—*Hepatic plasma flow rate. Data sources:* ○, Reference 20, *pp. 128, 129;* ×, Reference 22, *p. 244;* □, Reference 21, *p. 641; and* △, Reference 21, *p. 1405.*

This seemed too small compared to the more common 5000 ml., so the final equation used is adjusted by the ratio 5000/3500. For an average hematocrit of 40%, then:

$$V_P = (0.6)(5000/3500)(0.055)(1000W)^{0.99} = 44W^{0.99} \quad \text{(Eq. A1)}$$

At the other end of the scale, V_P for a 22-g. mouse ($W = 0.022$) is then 1 ml., which is the value used in the previous work (1).

The other relations are:

$$V_L = 0.082(1000W)^{0.87} = 34W^{0.87} \quad \text{(Eq. A2)}$$

$$V_K = 0.0212(1000W)^{0.85} = 7.5W^{0.85} \quad \text{(Eq. A3)}$$

$$V_M \simeq {}^1/_2(1000W) = 500W \quad \text{(Eq. A4)}$$

Adolph (17) gave the stomach and intestine weight as $0.112(1000W)^{0.94}$. Since the present model considers the small intestine only as the participating organ, two-thirds of the weight was used:

$$V_G = {}^2/_3(0.112)(1000W)^{0.94} = 49W^{0.94} \quad \text{(Eq. A5)}$$

These obviously somewhat arbitrary relations correspond reasonably well with commonly accepted values. It was found in previous work that consistency of values for the organ volumes is more important than absolute accuracy, which is the reason for devising the general equations.

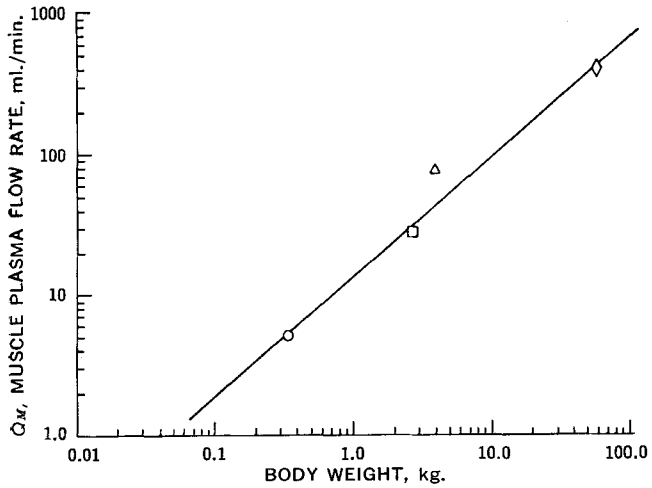

Figure A3—*Muscle plasma flow rate. Data sources:* ○, Reference 23; □, Reference 22, *p. 861;* △, Reference 24; *and* ◇, Reference 18.

With regard to flows, Fig. A1 shows data on renal plasma flow rate as a function of body weight on log–log paper to illustrate relationships in the form used by Adolph (17). The line is arbitrarily drawn through the data; it is also bracketed by Adolph's relations of *para*-aminohippuric acid and iodopyracet[1] clearances and should be reliable.

Figure A2 presents hepatic plasma flow rate. The data here are more scattered, but a reasonably good general estimate is evident. Limited available information on muscle perfusion rate is shown in Fig. A3. Much less data were readily available for the gut flow rate, and they were all for large animals. Based on these, a rough estimate of 0.8–0.85, or 0.82, of the hepatic flow rate was used (*Reference 20*, p. 1443; *Reference 22*, p. 244).

In the calculation of the flow rates for Figs. A1–A3, total plasma flow rates to the three compartments are calculated, as required, on the basis of a hematocrit of 0.40 and organ weight-to-body weight relationships.

REFERENCES

(1) K. B. Bischoff, R. L. Dedrick, and D. S. Zaharko, *J. Pharm. Sci.*, **59,** 149(1970).

(2) R. L. Dedrick and K. B. Bischoff, *Chem. Eng. Progr. Symp., Ser. 84*, **64,** 32(1968).

(3) K. B. Bischoff and R. L. Dedrick, *J. Pharm. Sci.*, **57,** 1346 (1968).

(4) D. S. Zaharko, R. L. Dedrick, and V. T. Oliverio, *Fed. Proc.*, **29,** 411(1970).

(5) D. M. Himmelblau and K. B. Bischoff, "Process Analysis and Simulation," Wiley, New York, N. Y., 1968.

(6) K. B. Bischoff, R. L. Dedrick, D. S. Zaharko, and S. Slater, *Proc. Ann. Conf. Eng. Med. Biol.*, **12,** 89(1970).

(7) G. W. Hepner, *Brit. J. Haematol.*, **16,** 241(1969).

(8) A. S. V. Burgen and N. J. Goldberg, *Brit. J. Pharmacol.*, **19,** 313(1962).

(9) I. D. Goldman, N. S. Lichtenstein, and V. T. Oliverio, *J. Biol. Chem.*, **243,** 5007(1968).

(10) D. S. Zaharko, H. Bruckner, and V. T. Oliverio, *Science*, **166,** 887(1969).

(11) W. C. Werkheiser, *J. Biol. Chem.*, **236,** 888(1961).

(12) E. S. Henderson, R. H. Adamson, and V. T. Oliverio, *Cancer Res.*, **25,** 1018(1965).

(13) C. J. McDonald and J. R. Bertino, *Lancet*, **1,** 864(1968).

(14) D. G. Johns, R. P. Spencer, P. K. Chang, and J. R. Bertino, *J. Nucl. Med.*, **9,** 530(1968).

(15) D. G. Liegler, E. S. Henderson, M. A. Hahn, and V. T. Oliverio, *Clin. Pharmacol. Ther.*, **10,** 849(1969).

(16) M. R. Sikov, J. M. Thomas, and D. D. Mahlum, *Growth*, **33,** 57(1969).

(17) E. F. Adolph, *Science*, **109,** 579(1949).

(18) W. W. Mapleson, *J. Appl. Physiol.*, **18,** 197(1963).

(19) G. Crile and D. P. Quiring, *Ohio J. Sci.*, **40,** 219(1940).

(20) "Handbook of Circulation," P. L. Altman, D. S. Dittmer, and R. M. Grebe, Eds., Saunders, Philadelphia, Pa., 1959.

(21) "Handbook of Physiology," W. F. Hamilton and P. Dow, Eds., American Physiological Society, Washington, D. C., 1962, sect. 2.

(22) "Medical Physics," vol. II, O. Glasser, Ed., Year Book Publishers, Chicago, Ill., 1950.

(23) T. T. Vogel, *Cardiologia*, **53,** 19(1968).

(24) R. F. Edlich, J. Borner, and R. J. Buchin, *Arch. Surg.*, **98,** 233(1969).

ACKNOWLEDGMENTS AND ADDRESSES

Received February 16, 1971, from the **Biomedical Engineering and Instrumentation Branch, Division of Research Services, and* †*Laboratory of Chemical Pharmacology, National Cancer Institute, National Institutes of Health, Public Health Service, U. S. Department of Health, Education, and Welfare, Bethesda, MD 20014*

Accepted for publication March 15, 1971.

‡ Present address: School of Chemical Engineering, Cornell University, Ithaca, NY 14850

[1] Diodrast.